

DTIC FILE COPY

Reprinted from JOURNAL OF PHYSICAL OCEANOGRAPHY, Vol. 18, No. 6, June 1988
American Meteorological Society

DTIC
ELECTE
OCT 04 1988
S D
H

AD-A204 017

The Fusion of Isolated Nonlinear Eddies

DORON NOF

Department of Oceanography and the Geophysical Fluid Dynamics Institute, The Florida State University, Tallahassee

(Manuscript received 22 April 1986, in final form 11 December 1987)

An inviscid nonlinear model is used to examine the

ABSTRACT

The interaction of two isolated lens-like eddies is examined with the aid of an inviscid nonlinear model. The barotropic layer in which the lenses are embedded is infinitely deep so that there is no interaction between the eddies unless their edges touch each other. It is assumed that the latter is brought about by a mean flow which relaxes after pushing the eddies against each other and forming a "figure 8" structure.

Using qualitative arguments (based on continuity and conservation of energy along the eddies' edge) it is shown that, once a "figure 8" shape is established, intrusions along the eddies' peripheries are generated. These intrusions resemble "arms" or "tentacles" and their structure gives the impression that one vortex is "hugging" the other. As time goes on the tentacles become longer and longer and, ultimately, the eddies are entirely converted into very long spiral-like tentacles. These spiraled tentacles are adjacent to each other so that the final result is a single vortex containing the fluid of the two parent eddies. It is speculated that the above process leads to the actual merging of lens-like eddies in the ocean.

Because of the inherent nonlinearity and the fact that the problem is three-dimensional (x, y, t), the complete details of the above process cannot be described analytically. Therefore, one cannot prove in a rigorous manner that the above process is the only possible merging mechanism. It is, however, possible to rigorously show analytically and experimentally that the intrusions and tentacles are inevitable. For this purpose, one of the interacting eddies is conceptually replaced by a solid cylinder. Initially, the cylinder drifts toward the eddy; subsequently, it is pushed slightly into the eddy and is then held fixed. The subsequent events are examined in a rigorous mathematical and experimental manner.

It is found that as the cylinder is forced into the eddy, a band of eddy water starts enveloping the cylinder in the clockwise direction. This tentacle continues to intrude along the cylinder parameter until it ultimately reattaches itself to the eddy, forming a "padlock" flow. Simple laboratory experiments on a rotating table clearly demonstrate that a "padlock" flow is indeed established when a lens is interacting with a solid cylinder. Using the details of this process it is argued that, in the actual eddy-eddy interaction case, intrusions must be established and that, consequently, merging of the two eddies is inevitable.

Reprints (edc)

DISTRIBUTION STATEMENT
Approved for public release
Distribution Unlimited

1. Introduction

Isolated lens-like eddies are common in many parts of the ocean; they usually result from meandering currents which close upon themselves and pinch-off (e.g., see The Ring Group 1981; Lai and Richardson 1977; Cheney 1977). Their abundance in the ocean and the, almost permanent, presence of mean currents suggest that collisions of lenses are probably a fairly common occurrence. The processes associated with such collisions and the resulting encounters are the focus of the present study.

a. Background

So far, there has been only one set of observations of a direct eddy-eddy interaction (Cresswell 1982; Cresswell and Legeckis 1986). In this case, two anticyclonic lens-like eddies have collided in the vicinity

of the East Australian Current. Initially, they moved around each other but within a period of about 20 days they have completely merged (Fig. 1). These observations have generated the interest of Gill and Griffiths (1981) who, in a short communication, have pointed out that if two inviscid eddies with zero potential vorticity are forced to merge and conserve their potential vorticity and mass during the merging, then the final vortex would have energy that is larger than the sum of the individual energies.

Consequently, it is concluded that, in order for mass-conserving merging to occur, either energy must be supplied from an outside source, or that potential vorticity is not conserved. The experiments of Nof and Simon (1987) have demonstrated that lenses merge without an external source of energy so that their potential vorticity must somehow be altered.

For additional studies on eddies interaction the reader is referred to Mied and Lindemann (1984), McWilliams (1983), McWilliams and Zabusky (1982), Overman and Zabusky (1982), Melander et al. (1987), and Christiansen and Zabusky (1973). While being informative, the latter investigations are not directly

Corresponding author address: Prof. Doron Nof, Dept. of Oceanography, Florida State University, Tallahassee, FL 32306.

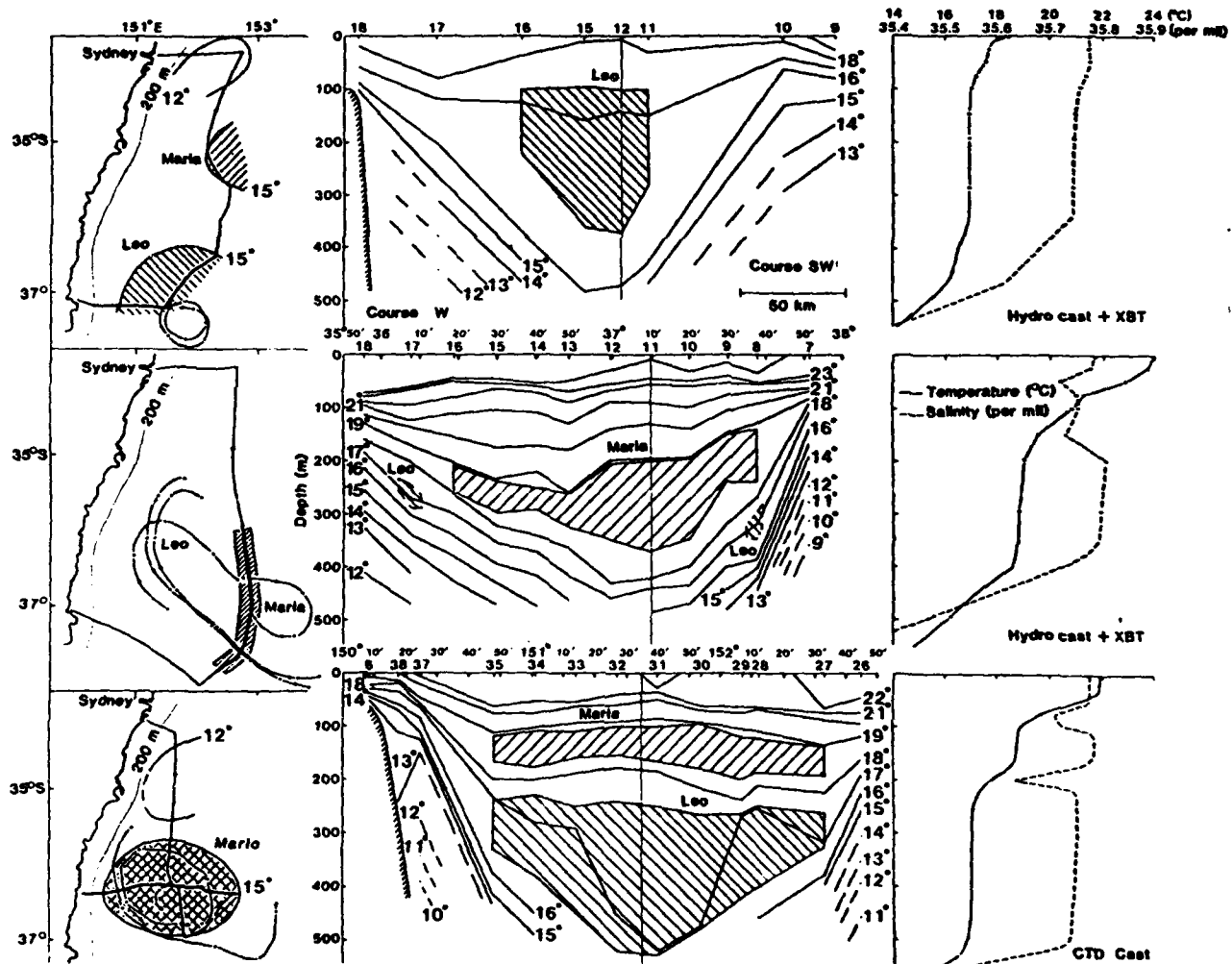


FIG. 1. The merging of two anticyclonic eddies off East Australia (adopted from Cresswell 1982). The results of Cresswell's ship surveys for December 1980, January 1981 and April 1981 are shown on top, middle, and bottom (respectively). In column 1 buoy tracks for several days before and after the surveys are marked; regions having 250-m temperatures exceeding 15°C are shaded; the 12°C isotherm for 250 m is marked. The thickened ship tracks define the temperature sections (in degrees Celsius) in column 2 where the signature layers of eddies Leo and Maria are shaded. The vertical lines in column 2 indicate the positions for the temperature and salinity profiles of column 3.

applicable to the problem at hand because they do not address lens-like eddies. The reader is also referred to the laboratory experiments of Griffiths and Hopfinger (1986, 1987) and the analysis of Young (1985) which discuss the interaction of quasi-geostrophic and geostrophic vortices. These eddies differ from our vortices because the latter are of finite extent whereas the former are infinite. That is to say, the eddies interactions which have been considered so far have an orbital speed that falls off as $1/r$ so that two eddies sense each other *no matter how far apart they are*. The presently considered lens-like eddies, on the other hand, do not sense each other unless they are in direct contact because dynamically they are identical to isolated blobs situated on top of a *dry* horizontal plate.

The purpose of the present paper is to explore analytically some of the details of the merging process. We will not be able to rigorously analyze the complete process and all its details (such as the actual alteration of potential vorticity) but we will be able to provide some information on the coalescence (i.e., the establishment of arms and tentacles).

b. Methods

The reader is warned in advance that part of the theory is qualitative and speculative in nature. The core of the theory (i.e., the so-called "padlock" flow), however, is a rigorous mathematical and experimental analysis. The general details of the proposed merging

mechanism are as follows. Two isolated blobs are initially separated from each other; they are embedded in a lighter (or heavier) infinitely deep layer so that, initially, one vortex does not "feel" the presence of its counterpart. The eddies are then brought together by some mean flow which relaxes after it pushes one vortex against the other. This creates a "figure 8" structure with a mutual boundary along which the depth does not vanish (Fig. 2). We shall see that because of the establishment of such a mutual boundary, the eddies cannot remain separated. "Tentacles" are extended from one vortex to another and rapid merging occurs.

Following the conclusion of Nof and Simon (1987) we develop a theory that corresponds to a situation where the final potential vorticity of the merged vortex is not identical to the initial potential vorticity which each vortex has had. The details of our proposed merging mechanism involve two main processes. The first is the way in which each of the two vortices becomes entangled in the "tentacles" of its counterpart and the second is the associated change in the potential vorticity. The former can be rigorously explained in terms

of relatively simple dynamical considerations whereas the causes of the latter are somewhat speculative. It is suspected that the change in potential vorticity is a result of shock waves that are present during the transient merging process.

Both processes are highly nonlinear; the interfaces of the blobs strike the surface (or bottom) so that the depth variations are of $O(1)$ and the centrifugal acceleration is of the same order as the Coriolis force so that the Rossby number is also of $O(1)$. Because of this and the fact that the general problem is three-dimensional (x, y, t) , it is impossible to describe all its details analytically. It is, however, possible to prove analytically that the formation of tentacles is inevitable; namely, it is possible to show that once a "figure 8" and a mutual boundary are established then each vortex must extend an "arm" around its counterpart (Fig. 3). To show this, one of the vortices is, conceptually, replaced by a solid cylinder and the flow resulting from slightly forcing the cylinder into the remaining eddy is examined. Note that since our model is inviscid it makes no difference whether or not the solid cylinder is rotating.

The main idea behind the above simplification is that both an adjacent eddy and an adjacent cylinder are forcing a mutual boundary along which the *depth does not vanish*. A similar simplification was used by Nof (1986a) to describe the collision between the Gulf Stream and a warm-core ring. However, there are two important differences between the Nof analysis and the present model. The first is that while curvature effects are very important in the present study, they are entirely negligible in the Nof (1986a) case. The second is that in the present case the volume of the fluid surrounding the cylinder is finite whereas in the Nof study there is a continuous flow from one area to another. These differences make the present study considerably more difficult than that discussed in Nof (1986a). Despite these differences, many of the techniques used in the above study are also applied here. There is some (but limited) overlapping between the two articles because an attempt has been made to make the present paper self-contained.

Because of the nonvanishing depth along the area in which the fluid is in direct contact with the cylinder, an intrusion of eddy water along the cylinder's perimeter is established. It propagates in a clockwise manner until it ultimately reaches the eddy on the downstream side. At this point the intrusion reattaches itself to the eddy and the combined eddy-intrusion flow resembles the shape of a padlock. Because of reattachment the "padlock" flow is steady and, even though the problem is still nonlinear, it is possible to obtain an analytical solution. This can be achieved by using a constraint resulting from integrating the equations representing the torque relative to the center of the cylinder. Much of the analysis and discussion in the paper is devoted to the padlock flow. The mere existence of a nonvan-

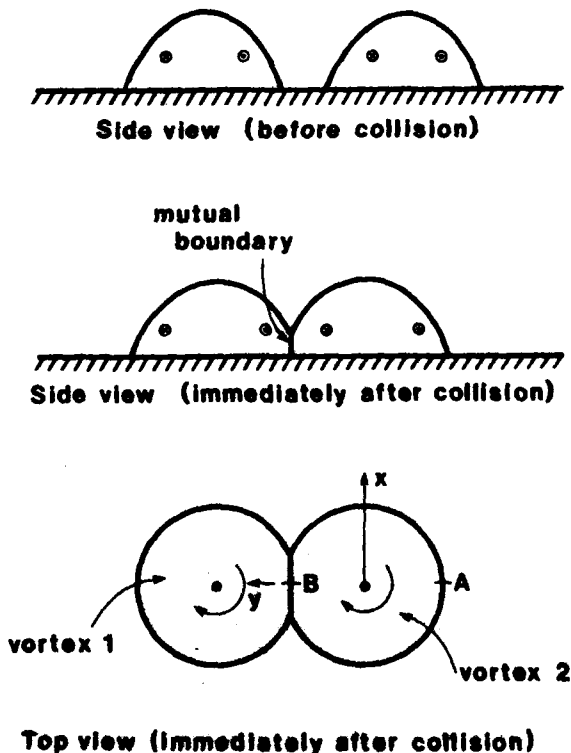


FIG. 2. Schematic diagram of the interaction of two isolated lens-like eddies. A side view of the eddies prior to any contact is shown on top. The middle and lower panels display the side and top views of two eddies which are touching each other due to, say, an advective current. The shape shown in the lower panel is referred to as the "figure eight" structure.

Original contains color plates: All DTIC reproductions will be in black and white.



A-1 001

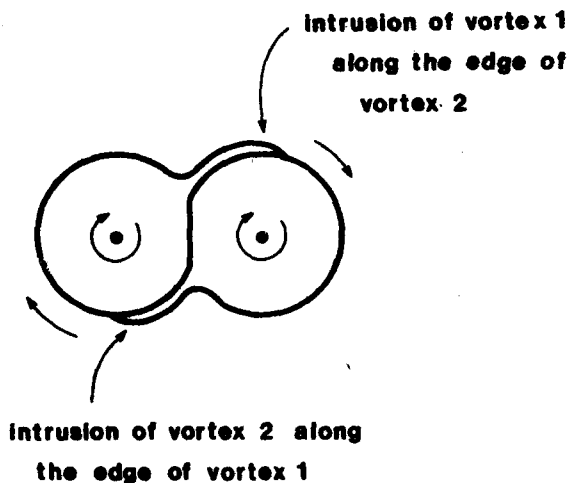


FIG. 3. The beginning of the double intrusion along the edges of the eddies.

ishing padlock flow illustrates that intrusion of eddy water along the cylinder is inevitable. We shall see that, consequently, one is led to the conclusion that interleaving and merging must take place. The padlock theory is supported by a series of laboratory experiments on a rotating table.

This paper is organized as follows. In section 2 the general structure of the merging process is described in detail; this description is largely qualitative. The simplification of the processes in question and the equations governing the padlock flow are given in section 3. Section 4 contains the appropriate scaling, and section 5 includes the solution for the padlock flow. The laboratory experiments are described in section 6. The results are discussed in section 7 and summarized in section 8. A list of symbols is given in the Appendix.

2. A qualitative description of the merging process

The material presented in this section is mostly descriptive and somewhat speculative. Consider again the two isolated blobs shown in Fig. 2. The blobs have uniform density and the slightly lighter fluid in which they are embedded is infinitely deep. Initially, the blobs do not touch each other so that there is no repulsion or attraction.

Suppose now that some mean flow has brought the two eddies together so that the eddies' horizontal projection resembles the "figure 8" shape and a mutual boundary is established (Fig. 2); after this happens the mean flow relaxes. Our initial intuition tells us that the eddies' response to the establishment of such a mutual boundary may simply consist of a localized adjusted flow in the vicinity of point B. However, a close examination of the problem shows that this is *not* the case. To show this, consider an application of the Ber-

noulli integral to the streamline connecting points A and B assuming, temporarily, that the flow is steady so that the eddies' response (to the establishment of a mutual boundary) consists indeed of a mere adjustment in the vicinity of point B,

$$u_A^2/2 = u_B^2/2 + g'h_B, \quad (2.1)$$

where u_A is the upstream speed¹ (in the x direction) along the front (point A), and u_B and h_B are the speed and depth at B.

Since h_B is always positive, (2.1) implies that $u_B < u_A$. However, if the steady response is in the manner shown in the lower panel of Fig. 2, as we have temporarily assumed, then continuity implies that there must be some convergence across the line connecting point B and the center of the vortices. This suggests that $u_B > u_A$. The above conditions, required by the continuity equation and the Bernoulli principle, are obviously incompatible, suggesting that there cannot be a streamline connecting A and B. Instead, it is expected that there will be a band of water flowing around the eddies in a clockwise manner (Fig. 3). In other words, particles moving along the vortex edge (i.e., the front) do not have sufficient energy to rise to point B and, therefore, must go around their adjacent vortex where the fluid is lower.

A formal proof for the inevitable existence of the edge intrusion is given in the following sections with aid of the so-called padlock flow. However, it should be pointed out that for the special case corresponding to $u_A = 0$ (i.e., a vortex with a zero speed along the edge) no proof is really necessary because under such conditions (2.1) can never be satisfied. The establishment of tentaclelike edge intrusions along the rims of both eddies creates a structure similar to that displayed in Fig. 4a. As time goes on the tentacles become longer and longer. Since the volume of each vortex is finite the tentacles will ultimately form a single vortex consisting of two adjacent spirals (Fig. 4b).

By equating the volume of each individual blob to the amount of water drained via the lengthening of the tentacles it is possible to estimate the total merging time. Specifically, suppose that ϵR_d denotes the distance that each vortex is initially "pushed" into its counterpart (where R_d is the deformation radius which is of the same order as the radius of the eddy) and that h denotes the eddy central depth. Also, recall that the intrusion advances in a similar fashion to a gravity current so that the propagation rate is of the order of the Kelvin wave speed $(\epsilon g'h)^{1/2}$ (e.g., see Griffiths 1986). With the aid of this information, we can now equate the volume of each eddy [$\sim O(R_d^2 h)$] to the intrusion flux [ϵR_d , the intrusion width, times the in-

¹ For clarity, the definition of symbols is given in both the text and an appendix.

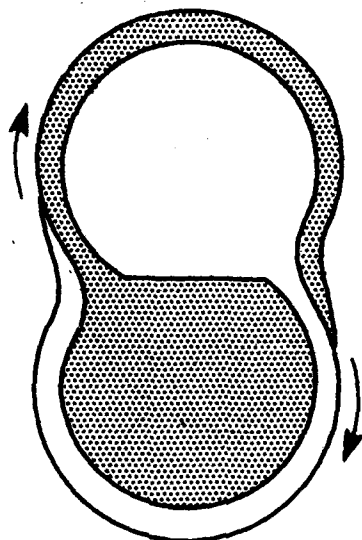


FIG. 4a. Schematic diagram of the edge intrusion in an advanced stage.

trusion depth $\sim O(\epsilon h)$ and the intrusion propagation speed $\sim O(\epsilon g' h)^{1/2}$ multiplied by the merging time (t_m). This gives,

$$t_m \sim O(f \epsilon^{3/2})^{-1} \quad (2.2)$$

which shows that if the relative distance that each vortex is "pushed" into the other is, say, 0.1 and the Coriolis parameter f is $\sim 10^{-4} \text{ sec}^{-1}$, then the merging time is roughly 30 days.

The above processes strongly suggest that merging will indeed take place. There remain, however, two important aspects that need to be addressed. The first is that we still need to rigorously prove that the intrusions are indeed inevitable. The second is that we need to explain how the potential vorticity is altered during the merging. The former aspect is rigorously discussed in sections 3-5 whereas the latter is qualitatively addressed below.

It is argued that the alteration of potential vorticity is probably achieved via the action of shock waves² in the nose of the intrusion. The fact that intrusions contain bores is not new. It was first pointed out by Benjamin (1968) for nonrotating flows. The laboratory experiments of Stern et al. (1982), Griffiths and Hopfinger (1983), and Kubokawa and Hanawa (1984), and the analysis presented by Simpson (1982) and Griffiths (1986) suggest that rotating intrusions along straight coastlines also contain shock waves.

Also, the study of Nof (1987) has demonstrated that the absence of shock waves in an intrusion along a

coast is only possible under rather special conditions. That is, it has been demonstrated that steadily propagating solutions which do not involve shock waves are only possible for specific circumstances. These special solutions are not the most general solution to the problem which must involve steepening and dissipation associated with depth discontinuities. In an independent study, Nof (1986b) has demonstrated that rotating shock waves cause a major alteration of potential vorticity. We, therefore, speculate that, as the fluid is intruding along the adjacent vortex edge, its potential vorticity is altered.

Note that, during the merging, *all* the fluid in the vortices is processed by the shocks so that the potential vorticity of all the fluid is altered. Griffiths and Hopfinger (1987) argue that this was not the case in their merging experiment. They contend that in their linear eddies only a small fraction of the fluid could be processed by the shock. While this could have been the case in their experiments, intrusions with zero potential vorticity such as ours will process all the fluid contained in the vortex. This can be easily seen by examining the system in a coordinate system moving with the intrusion's nose. It is expected that in such a system, all the intruding fluid will circulate through the shock because the shear is of $O(1)$. Unfortunately, a quantitative detailed analysis of the shocks in the intrusion is quite complicated. It is beyond the scope of this study and will be the subject of a future investigation.

This completes our qualitative, and somewhat speculative, description of the merging processes. We now turn to the rigorous part of the analysis where the "padlock" flow is analyzed.

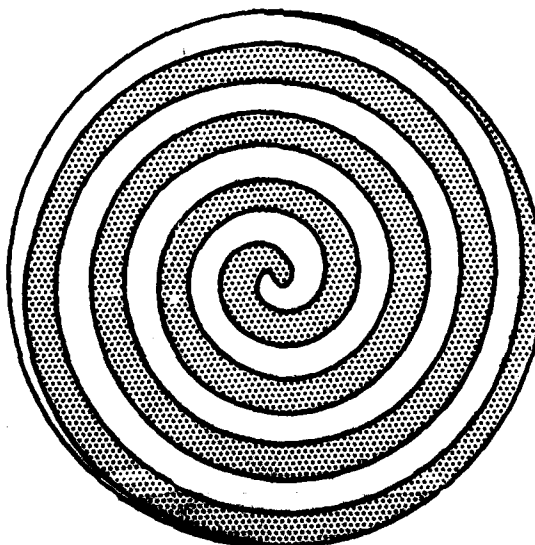


FIG. 4b. Schematic diagram of the edge intrusion in the final stage. Note that complete merging occurs because the intrusions "leak" all the fluids of the vortices.

² By "shock waves" (or bores) we mean organized depth discontinuities in which there is a violent turbulent action. They correspond to a balance between steepening and dissipative effects.

3. The steady "padlock" flow—governing equations and constraints

The present section has two aims. First, we want to show that the eddy's response to the presence of the cylinder cannot consist of a mere adjustment in the contact area (Fig. 5). Namely, we wish to prove that there must always be a flow around the cylinder so that the time dependent intrusion (Fig. 6a) is inevitable. The second aim is to find how the eddy responds to the forced cylinder. Specifically, one would like to compute the padlock flow speed, width and depth as a function of the distance that the cylinder is pushed into the eddy. Because of the inherent nonlinearity of the problem, which has not been removed by our simplification, it is unlikely that one will be able to find analytical solutions for the whole field. Consequently, we shall make an attempt to find the desired flow pattern without solving for the entire field.

a. General description

Consider the system shown in Fig. 6b. The origin of our coordinates system is located at the center of the cylinder; it will become clear later that this choice is

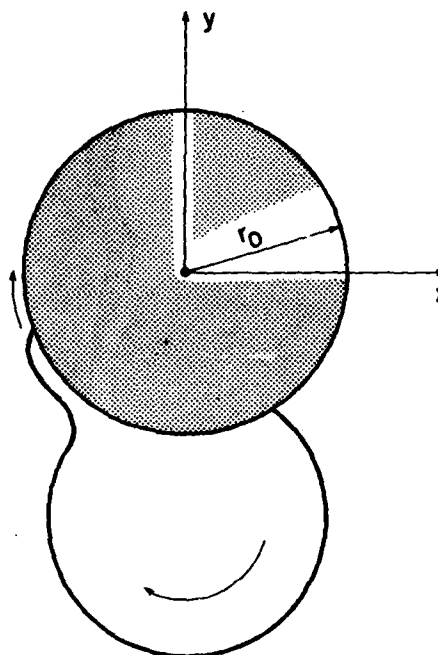


FIG. 6a. The initial intrusion stage. Ultimately, the intrusion reattaches itself to the eddy and a steady "padlock" flow is established.

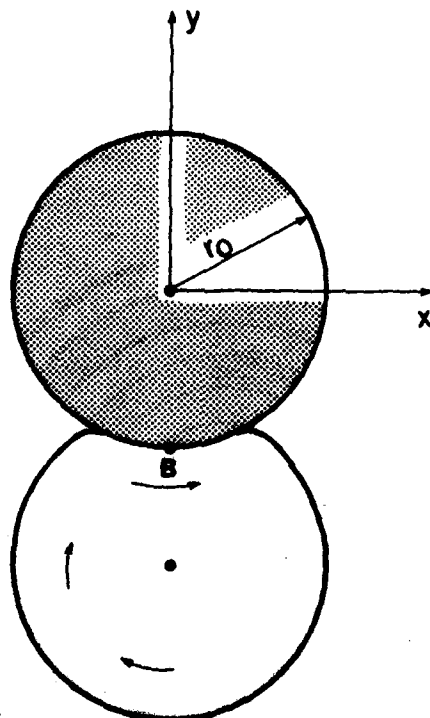


FIG. 5. A schematic diagram of a hypothetical response to a forced cylinder. The vortex is adjacent to the solid cylinder which has been slightly forced into it. The diagram illustrates an adjustment which is confined to the contact area; as shown in the text such a situation cannot exist. Instead, there must be an intrusion around the cylinder (Fig. 6a) so that, ultimately, a "padlock" flow is established (Fig. 6b).

not arbitrary. The x axis is perpendicular to the line connecting the center of the cylinder with the center of the vortex; the y axis is a continuation of the above line and the system rotates uniformly at $f/2$ about the z axis. The padlock flow is embedded in an infinitely deep motionless layer; its potential vorticity is zero. The way that the padlock flow is conceptually formed is not important for our analysis. It is useful to point out, however, that one can think of several ways by which it can be established. An obvious procedure is to physically force the cylinder into an eddy. Another method is to, conceptually, pull out a long tube (containing heavy fluid which is not, necessarily, at rest) in the neighborhood of a solid cylinder. A third method would be to inject the heavy fluid near the bottom of the cylinder.

Whatever generation method is used, there will be some period of adjustment, and ultimately, a steady flow will be established. At this final stage (Fig. 6b) the boundary of the solid cylinder extends beyond the boundary of a zero potential vorticity eddy whose depth and center are aligned with those of the padlock flow. We define this latter vortex to be our "undisturbed" eddy even though it is not necessarily identical to the initial lens due to the time dependent processes.

As stated, the manner in which the padlock flow is established is not important for the present analysis. What we wish to find out is whether or not the final adjusted state can only be associated with a padlock

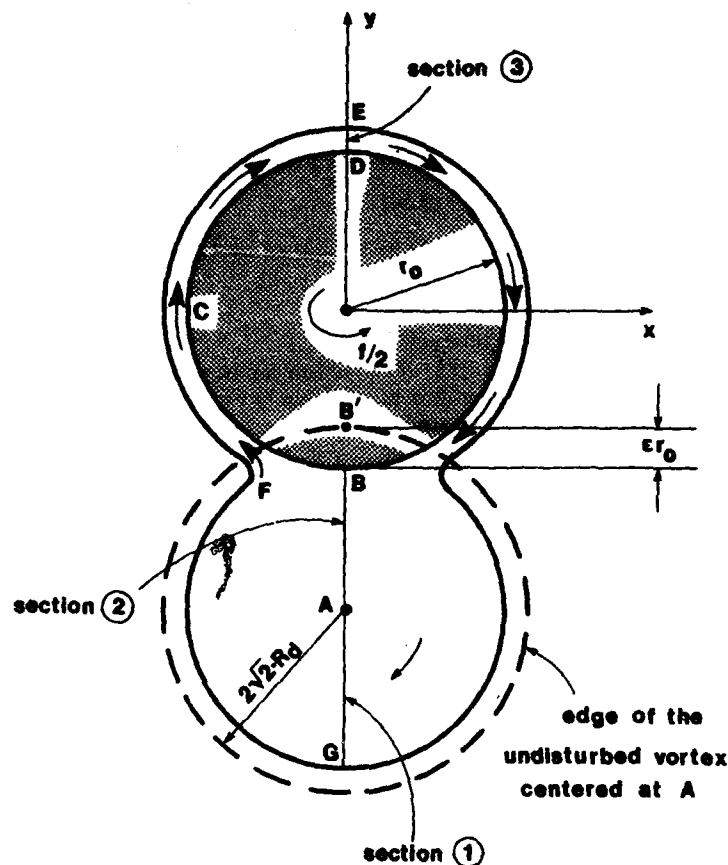


FIG. 6b. Schematic diagram of the "padlock" flow. Point A is defined as the point at which the speed of the padlock flow vanishes; h is the depth at A and the radius of the undisturbed vortex (which is centered at A and has a maximum depth \hat{h}) is $2\sqrt{2}R_d$ [where $R_d = (g'h)^{1/2}/f$].

flow. Namely, we ask the following question: Is there a solution corresponding to a mere adjustment in the contact area? The answer to the latter question would be positive if the width of the padlock flow turns out to be zero. We shall see that this is *not* the case; i.e., we shall see that there must be a flow around the cylinder whenever the edge of the undisturbed vortex extends beyond the surface of the cylinder ($\epsilon \neq 0$).

b. Governing equations for sections 1, 2 and 3

The governing equations for the final adjusted state are the usual shallow water equations. For a padlock flow with zero potential vorticity we have,

$$\partial v_i / \partial x - \partial u_i / \partial y + f = 0, \quad i = 1, 2, 3 \quad (3.1a)$$

$$u_i \frac{\partial v_i}{\partial x} + v_i \frac{\partial v_i}{\partial y} + f u_i = -g' \frac{\partial h_i}{\partial y}, \quad i = 1, 2, 3 \quad (3.1b)$$

$$\frac{\partial}{\partial x} (h u_i) + \frac{\partial}{\partial y} (h v_i) = 0, \quad i = 1, 2, 3 \quad (3.1c)$$

where u and v are the horizontal depth-independent velocity components in the x and y direction, and the subscripts 1, 2 and 3 denote that the variable in question is associated with sections 1, 2 and 3, respectively. Note that because of the symmetry of the problem (i.e., $v = 0, h_x = 0$ along cross sections 1, 2 and 3) the x momentum equation [$\partial u_i / \partial x + v_i (\partial u_i / \partial y) - f v_i = -g' (\partial h / \partial x)$] and the continuity equation (3.1c) imply that

$$\frac{\partial u_i}{\partial x} = 0. \quad (3.2)$$

In addition, note that, as in many radially symmetric eddies, $\partial v_i / \partial x$ is *not* necessarily zero where $x = 0$ even though $v = 0$.

The boundary conditions for sections 1, 2 and 3 are

$$h_1 = 0; \quad y = -r_0(1 - \epsilon) - 4\sqrt{2} \cdot R_d - 2\sqrt{2} \cdot R_d(1 - \gamma_1) \quad (3.3a)$$

$$h_1 = \hat{h}; \quad y = -r_0(1 - \epsilon) - 2\sqrt{2} \cdot R_d \quad (3.3b)$$

$$u_1 = v_1 = 0; \quad y = -r_0(1 - \epsilon) - 2\sqrt{2} \cdot R_d \quad (3.3c)$$

$$[u_1^2]_{y=-r_0(1-\epsilon)-2\sqrt{2} \cdot R_d}^{y=r_0(1+\gamma_3)} = [u_3^2]_{y=r_0(1+\gamma_3)} \quad (3.4)$$

$$[u_2^2 + 2g'h_2]_{y=-r_0} = [u_3^2 + 2g'h_3]_{y=r_0} \quad (3.5a)$$

$$h_2 = \hat{h}; \quad y = -r_0(1 - \epsilon) - 2\sqrt{2} \cdot R_d \quad (3.5b)$$

$$u_2 = v_2 = 0; \quad y = -r_0(1 - \epsilon) - 2\sqrt{2} \cdot R_d \quad (3.5c)$$

$$h_3 = 0; \quad y = r_0(1 + \gamma_3), \quad (3.6)$$

where r_0 is the radius of the cylinder and R_d is the deformation radius based on the depth at the center of the padlock flow (i.e., where the speed vanishes) so that the radius of the undisturbed vortex is $2\sqrt{2} \cdot R_d$. The γ_1 and γ_3 denote nondimensional locations at which the depths of the flow in sections 1 and 3 vanish (Fig. 6b). Conditions (3.3a) and (3.6) state that the depth of these flows vanishes at some unknown location; conditions (3.4) and (3.5a) reflect the conservation of energy along the streamlines that bound the flow from left and right (looking downstream). Namely, (3.4) and (3.5a) are simply a result of an application of the Bernoulli integral to the streamlines connecting G and E, and B and D (see Fig. 6b). Conditions (3.3b) and (3.5b) state that at A the depths of the two sections are identical to some given depth (\hat{h}) and (3.3c) and (3.5c) reflect the requirement for a vanishing speed at the center of the vortex.

It is important to distinguish clearly between the undisturbed state and the initial state. As mentioned before, the undisturbed vortex is defined as a zero potential vorticity vortex which is centered at the center of the padlock flow (i.e., the point where the velocity vanishes) and has the same depth as the maximum padlock flow (\hat{h}); its radius is $2\sqrt{2} \cdot R_d$. The initial state, on the other hand, is the state which leads to the intrusion and the padlock flow—of no interest for the present study.

c. Constraints

The flows in the various sections are connected to each other via (3.4) and (3.5) but there are two additional constraints that the unknown variables must satisfy. The first results simply from continuity and can be written in the form,

$$\int_G^A u_1 h_1 dy + \int_A^B u_2 h_2 dy + \int_D^E u_3 h_3 dy = 0. \quad (3.7)$$

The second equation will be derived from the conservation of torque. As in Nof (1986a), we begin by noting that the moment of momentum corresponds to the cross-product of the position vector r and the momentum equations,

$$y \left(u \frac{\partial u}{\partial x} + v \frac{\partial u}{\partial y} - f v + g' \frac{\partial h}{\partial x} \right) - x \left(u \frac{\partial v}{\partial x} + v \frac{\partial v}{\partial y} + f u + g' \frac{\partial h}{\partial y} \right) = 0. \quad (3.8)$$

To show that (3.8) provides an additional connection between sections 1, 2 and 3, it is multiplied by h and the continuity equation (3.7a) is incorporated. This gives

$$\frac{\partial}{\partial x} (hu^2y) + y \frac{\partial}{\partial y} (huv) - fvyh + \frac{g'}{2} \frac{\partial}{\partial x} (h^2y) - x \frac{\partial}{\partial x} (huv) - \frac{\partial}{\partial y} (h xv^2) - fuhx - \frac{g'}{2} \frac{\partial}{\partial y} (h^2x) = 0, \quad (3.9)$$

which can be rearranged and integrated over the region shown in Fig. 7, to give

$$\int_{-\infty}^{+\infty} \frac{\partial}{\partial x} \left(hu^2y - f\psi y + \frac{g'}{2} h^2y - huvx \right) dx dy + \int_{-\infty}^{+\infty} \frac{\partial}{\partial y} \left(huvy + f\psi x - \frac{g'}{2} h^2x - h xv^2 \right) \times dx dy = 0 \quad (3.10)$$

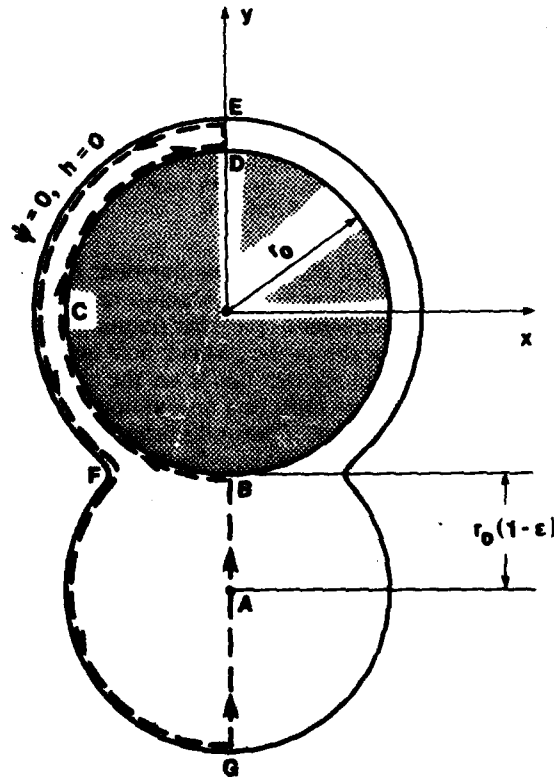


FIG. 7. An illustration of the integration area for the computation of the torque associated with the padlock flow.

where ψ is a streamfunction defined by

$$\frac{\partial \psi}{\partial y} = -uh; \quad \frac{\partial \psi}{\partial x} = vh. \quad (3.11)$$

By using Stokes' theorem, (3.11) can be written in the form,

$$\oint_{\phi} \left(hu^2 y - f\psi y + \frac{g'}{2} h^2 y - huvx \right) dy - \oint_{\phi} \left(huvy - hxv^2 + f\psi x - \frac{g'}{2} h^2 x \right) dx = 0. \quad (3.12)$$

where ϕ is the boundary of the flow. This equation can be further simplified by defining ψ to be zero along the edge where $h = 0$ and noting that along any streamline $udy = vdx$. This gives,

$$\begin{aligned} & \int_G^B (hu^2 - f\psi + g'h^2/2) y dy \\ & + \int_D^E (hu^2 - f\psi + g'h^2/2) y dy \\ & + \int_B^D (-f\psi y + g'h^2 y/2) dy \\ & - \int_B^D (f\psi x - g'h^2 x/2) dx = 0. \quad (3.13) \end{aligned}$$

In deriving (3.13) it has been taken into account that the sum of the integrals of $hu^2 y$ and $huvy$ along BD vanishes because there is no normal flow through the boundary of the cylinder.

The first two terms in (3.13) are the moments of the flow force in sections 1, 2 and 3. The last two terms, on the other hand, represent the torque corresponding to the pressure exerted on the cylinder by the surrounding flow. Since we chose our origin to be in the center of the cylinder and the pressure is always perpendicular to the surface with which the fluid is in contact, we would expect this torque to vanish. It is easy to show that since the cylinder surface is given by $x^2 + y^2 = r_0^2$, we have $x dx + y dy = 0$ so that the sum of the last two integrals in (3.13) equals zero as expected. Hence, the integrated torque takes the simple form,

$$\begin{aligned} & \int_G^A (h_1 u_1^2 - f\psi_1 + g'h_1^2/2) y dy \\ & + \int_A^B (h_2 u_2^2 - f\psi_2 + g'h_2^2/2) y dy \\ & + \int_D^E (h_3 u_3^2 - f\psi_3 + g'h_3^2/2) y dy = 0, \quad (3.14) \end{aligned}$$

where we have incorporated our special notation for the various sections.

4. Scaling and expansion of the padlock flow

a. The basic state

Before discussing the scaling of the problem and the general structure of the expansion, it is instructive to look at the details of the basic state. The structure of the zero-order state, corresponding to the cylinder "kissing" an eddy with zero potential vorticity, is not a priori obvious. To show this, consider the application of the Bernoulli integral to the surface of the cylinder (3.5). It implies that even when $\epsilon \rightarrow 0$ the velocity along the cylinder surface is of $O(1)$ because the eddy speed along the edge is $O(1)$ [see (1.1) with $r = 2(2g'h)^{1/2}/f$]. As in Nof (1986a), this means that the basic flow around the cylinder is not zero; rather, it consists of an infinitesimal ribbon flowing at a speed $(2g'h)^{1/2}$. To find the details of this ribbon flow it is noted that even though the basic state contains only an infinitesimal strip, it must, of course, satisfy the equations of motion.

In this context, it is convenient to consider the potential vorticity equation and momentum conservation in cylindrical coordinate (r, ϑ) ,

$$\frac{1}{r} \frac{d}{dr} (r\bar{v}_\vartheta) + f = 0 \quad (4.1)$$

$$\frac{\bar{v}_\vartheta^2}{r} + f\bar{v}_\vartheta = g' \frac{d\bar{h}}{dr}, \quad (4.2)$$

where \bar{v}_ϑ is the tangential velocity, the bar ($\bar{\quad}$) indicates association with the basic state and we have assumed that the basic flow is purely tangential (i.e., $\bar{v}_r = \partial/\partial\vartheta = 0$). The most general solution of (4.1) and (4.2) is

$$\begin{aligned} \bar{v}_\vartheta &= -\frac{fr}{2} + \frac{\alpha}{r}; \\ \bar{h} &= (r_0^2 - r^2) \frac{f^2}{8g'} + \left(\frac{1}{r_0^2} - \frac{1}{r^2} \right) \frac{\alpha^2}{2g'}, \quad (4.3) \end{aligned}$$

where α is an unknown constant and we have used the condition $\bar{h} = 0$ at $r = r_0$. Since at $r = r_0$ the absolute value of the velocity must be $(2g'h)^{1/2}$ (in order to satisfy the Bernoulli relationship along the surface of the cylinder), we find from (4.3) that

$$\alpha = \frac{fr_0}{2} (r_0 - 2\sqrt{2}R_d) \quad (4.4)$$

where $R_d = (g'h)^{1/2}/f$. Namely, for any given cylinder (r_0), we must take a specific value for α . For simplicity, we shall consider only cylinders with $r_0 = 2\sqrt{2}R_d$ so that $\alpha = 0$. Other cylinders can, of course, also be considered and the solution, which will be shortly derived, can be easily extended to cylinders with all diameters. However, such extended solutions do not provide any new physical insights and, therefore, are not presented.

b. Scaling

In the subsequent analysis the following nondimensional variables will be used:

$$\left. \begin{aligned} u^* &= u/(g'h)^{1/2}; & v^* &= v/(g'h)^{1/2}; \\ h^* &= h/h \\ x^* &= x/R_d; & y^* &= y/R_d; \\ r_0^* &= r_0/R_d = 2\sqrt{2}; & r^* &= r/R_d \\ \psi^* &= \psi/[g'(h)^2/f]; & R_d &= (g'h)^{1/2}/f \end{aligned} \right\} \quad (4.5)$$

Note that in sections 1 and 3, which are located far from the contact area, the flow is taken to be purely tangential. This is clearly supported by our laboratory experiment (section 6). In section 2, however, some deviations from radially symmetric motion are possible because of the presence of the cylinder. In view of this, we shall use polar coordinates for sections 1 and 3 and Cartesian coordinates for section 2. [The subscript ϑ will denote association with polar coordinates (i.e., v_ϑ is the azimuthal speed) whereas the lack of a subscript will indicate that the variable in question is associated with Cartesian coordinates.] For section 1 it is convenient to transfer the coordinate system and use cylindrical coordinates $(\tilde{r}, \tilde{\vartheta})$ situated at the center of the padlock flow $[0; -r_0(2 - \epsilon)]$. In terms of the nondimensional numbers defined by (4.5), the governing equations for this section are

$$\frac{1}{\tilde{r}} \frac{d}{d\tilde{r}} (\tilde{r} \tilde{v}_1) + 1 = 0; \quad (\tilde{v}_1)^2 / \tilde{r} + \tilde{v}_1 = \frac{d\tilde{h}_1}{d\tilde{r}} \quad (4.6a)$$

where $\tilde{r}, \tilde{\vartheta}$ are related to the original coordinates system (x^*, y^*) via,

$$\tilde{r} \sin \tilde{\vartheta} = y^* + 2\sqrt{2}(2 - \epsilon); \quad \tilde{r} \cos \tilde{\vartheta} = x^* \quad (4.6b)$$

[i.e., $\tilde{y} = y^* + 2\sqrt{2}(2 - \epsilon); \tilde{x} = x^*$]. For section 3 it is not advantageous to transfer the coordinates system. We, therefore, take,

$$\frac{1}{r^*} \frac{d}{dr^*} (r^* v_{\vartheta 3}^*) + 1 = 0; \quad (v_{\vartheta 3}^*)^2 / r^* + v_{\vartheta 3}^* = \frac{dh_3^*}{dr^*} \quad (4.6c)$$

The nondimensional equations for section 2 are found from (4.5) and (3.1) to be

$$\frac{\partial v_x^*}{\partial x^*} - \frac{\partial u_x^*}{\partial y^*} + 1 = 0 \quad (4.7a)$$

$$u_x^* \frac{\partial v_x^*}{\partial x^*} + u_y^* = -\frac{\partial h_2^*}{\partial y^*} \quad (4.7b)$$

$$\frac{\partial}{\partial x^*} (h_2^* u_x^*) = 0 \quad (4.7c)$$

where we have taken into account that $v_y^* = 0$ because of symmetry. (Note, however, that, as mentioned before, the terms containing $\partial v_x^* / \partial x^*$ are not necessarily zero even though $v_y^* = 0$.) The boundary conditions (3.3)–(3.6) take the form,

$$h_1^* = 0; \quad y^* = -2\sqrt{2}(3 - \epsilon - \gamma_1) \quad (4.8a)$$

$$h_1^* = 1; \quad y^* = -2\sqrt{2}(2 - \epsilon) \quad (4.8b)$$

$$u_1^* = v_1^* = 0; \quad y^* = -2\sqrt{2}(2 - \epsilon) \quad (4.8c)$$

$$[(u_1^*)^2]_{y^*=-2\sqrt{2}(3-\epsilon-\gamma_1)} = [(u_1^*)^2]_{y^*=-2\sqrt{2}(1+\gamma_3)} \quad (4.9)$$

$$[(u_1^*)^2 + 2h_1^*]_{y^*=-2\sqrt{2}} = [(u_1^*)^2 + 2h_1^*]_{y^*=-2\sqrt{2}} \quad (4.10a)$$

$$h_2^* = 1; \quad y^* = -2\sqrt{2}(2 - \epsilon) \quad (4.10b)$$

$$u_2^* = v_2^* = 0; \quad y^* = -2\sqrt{2}(2 - \epsilon) \quad (4.10c)$$

$$h_3^* = 0; \quad y^* = 2\sqrt{2}(1 + \gamma_3) \quad (4.11)$$

Similarly, the constraints (3.7) and (3.14) can be expressed as,

$$\int_{-2\sqrt{2}(3-\epsilon-\gamma_1)}^{-2\sqrt{2}(2-\epsilon)} u_1^* h_1^* dy + \int_{-2\sqrt{2}(2-\epsilon)}^{-2\sqrt{2}} u_2^* h_2^* dy^* + \int_{2\sqrt{2}}^{2\sqrt{2}(1+\gamma_3)} u_3^* h_3^* dy^* = 0 \quad (4.12)$$

$$\int_{-2\sqrt{2}(3-\epsilon-\gamma_1)}^{-2\sqrt{2}(2-\epsilon)} [h_1^* (u_1^*)^2 - \psi_1^* + (h_1^*)^2 / 2] y^* dy^* + \int_{-2\sqrt{2}(2-\epsilon)}^{-2\sqrt{2}} [h_2^* (u_2^*)^2 - \psi_2^* + (h_2^*)^2 / 2] y^* dy^* + \int_{-2\sqrt{2}}^{-2\sqrt{2}(1+\gamma_3)} [h_3^* (u_3^*)^2 - \psi_3^* + (h_3^*)^2 / 2] y^* dy^* = 0. \quad (4.13)$$

c. Perturbation expansion

As in Nof (1986a), the expansion in ϵ is not straightforward for two reasons. First, as already pointed out, the basic state ($\epsilon = 0$) contains speeds of $O(1)$. Second, the choice for the origin of the coordinates system implies that the basic flow is a function of ϵ . Recall that the choice of the origin for the coordinate system was "imposed" by the use of the integrated torque. If the origin were in any other location, then the integrated torque associated with the pressure along BCD would have remained nonzero thus making it impossible to connect the three sections. It will become clear shortly that while these conditions make the expansion somewhat more involved they do not present any fundamental difficulty.

It is assumed that, for sections 1 and 3, the expansion has the form,

$$\tilde{v}_1 = -\tilde{r}/2 + \epsilon \tilde{v}_1^{(1)} + \epsilon^2 \tilde{v}_1^{(2)} + \dots \quad (4.14a)$$

$$\tilde{h}_1 = 1 - (\tilde{r})^2/8 + \epsilon \tilde{h}_1^{(1)} + \epsilon^2 \tilde{h}_1^{(2)} + \dots \quad (4.14b)$$

$$\gamma_1 = \epsilon \gamma_1^{(1)} + \epsilon^2 \gamma_1^{(2)} + \dots \quad (4.14c)$$

$$v_{\vartheta 3}^* = -r^*/2 + \epsilon v_{\vartheta 3}^{(1)} + \epsilon^2 v_{\vartheta 3}^{(2)} + \dots \quad (4.15a)$$

$$h_3^* = 1 - (r^*)^2/8 + \epsilon h_3^{(1)} + \epsilon^2 h_3^{(2)} + \dots \quad (4.15b)$$

$$\gamma_3 = \epsilon \gamma_3^{(1)} + \epsilon^2 \gamma_3^{(2)} + \dots, \quad (4.15c)$$

where (4.3) and (4.5) have been used to express the terms corresponding to the basic state. Note that, as before, the tilde ($\tilde{}$) denotes association with a polar coordinates system whose origin is located at the center of the eddy instead of the center of the cylinder ($x^* = y^* = 0$). The relationship between \tilde{r} and x^* and y^* is easily found from (4.6b) to be,

$$\tilde{r} = \{(x^*)^2 + [y^* + 2\sqrt{2}(2 - \epsilon)]^2\}^{1/2}. \quad (4.15d)$$

As in Nof (1986a), the expansions (4.14)–(4.15) take into account that the width of the flow around the cylinder (γ_3) is $O(\epsilon R_d)$ because this is also the width of the flow blocked by the cylinder (i.e., section BB', Fig. 6b). In other words, the width of the flow in section 3 is of the order of the distance that the cylinder is "pushed" into the eddy. The depth near the cylinder boundary in section 3 must be of the same order as the depth at B because the blocked transport is $O(g'h_B^2/2f)$ and the transport at cross section 3 is $O(g'h_{3w}^2/2f)$, where h_{3w} is the depth near the wall at section 3. Namely, a Taylor series expansion (around the edge of the undisturbed eddy) for the depth at B shows that $h_B \sim O(\epsilon \tilde{h})$ and, consequently, $h_{3w} \sim O(\epsilon \tilde{h})$. These scales are consistent with the scales that one finds along the immediate vicinity of the rim of any lens-like eddy.

As mentioned, in section 2 the flow is not necessarily radially symmetric so that the expansion is

$$u_{\tilde{r}}^{\tilde{r}} = [y^* + 2\sqrt{2}(2 - \epsilon)]/2 + \epsilon u_2^{(1)} + \epsilon^2 u_2^{(2)} + \dots \quad (4.16a)$$

$$v_{\tilde{r}}^{\tilde{r}} = -x^*/2 + \epsilon v_2^{(2)} + \epsilon^2 v_2^{(2)} + \dots \quad (4.16b)$$

$$h_{\tilde{r}}^{\tilde{r}} = 1 - [y^* + 2\sqrt{2}(2 - \epsilon)]^2/8 + \epsilon h_2^{(1)} + \epsilon^2 h_2^{(2)} + \dots \quad (4.16c)$$

Recall now that because of our choice for the origin of (x^* , y^*), our basic state contains ϵ when it is expressed in terms of x^* and y^* . While this does not create any difficulties, it is perhaps more elegant to express (4.16a) and (4.16c) in the form,

$$u_{\tilde{r}}^{\tilde{r}} = [y^* + 4\sqrt{2}]/2 + \epsilon(u_2^{(1)} - \sqrt{2}) + \epsilon^2 u_2^{(2)} + \dots \quad (4.17a)$$

$$h_{\tilde{r}}^{\tilde{r}} = 1 - (y^* + 4\sqrt{2})^2/8 + \epsilon(h_2^{(1)} + y^*\sqrt{2}/2) + \epsilon^2(h_2^{(2)} - 1) + \dots \quad (4.17b)$$

In this form, the power series are expressed in a way that clearly separates the zero-order terms from the remaining terms. Hereafter, the first terms in (4.17) will be referred to as $u_2^{(0)}$ and $h_2^{(0)}$, respectively.

5. Solution for the padlock flow

a. General solution for section 1

Substitution of (4.14) into (4.6) and elimination of the terms corresponding to the basic state gives the $O(\epsilon)$ equation,

$$\frac{1}{\tilde{r}} \frac{d}{d\tilde{r}} (\tilde{r} \tilde{v}_{\phi}^{(1)}) = 0. \quad (5.1)$$

The solution is: $\tilde{v}_{\phi}^{(1)} = A_1/\tilde{r}$, where A_1 is an unknown constant. Since $\tilde{v}_{\phi}^{(1)}$ cannot approach infinity at the center of the vortex ($\tilde{r} = 0$) we find that

$$\tilde{v}_{\phi}^{(1)} = A_1 = 0 \quad (5.2)$$

and $\tilde{h}_1^{(1)} = B_1$ where B_1 is a constant to be determined. At the center of the vortex the depth \tilde{h} must match the undisturbed depth ($\tilde{h} = 1$) because of our definition of the basic state. Hence, we have $B_1 = 0$ and

$$\tilde{h}_1^{(1)} = 0. \quad (5.3a)$$

Also, with the aid of (4.8a) one obtains,

$$\tilde{\gamma}_1^{(1)} = 0. \quad (5.3b)$$

It is a simple matter to show that, in a similar fashion to the first-order solution, the second-order solution in section 2 also vanishes, i.e.,

$$\tilde{h}_1^{(2)} = \tilde{v}_{\phi}^{(2)} = \gamma_1^{(2)} = 0. \quad (5.3c)$$

b. Simplified equations for section 2

From (4.16) and (4.7) one finds the $O(\epsilon)$ equations,

$$\frac{\partial v_2^{(1)}}{\partial x^*} - \frac{\partial u_2^{(1)}}{\partial y^*} = 0 \quad (5.4a)$$

$$u_2^{(0)} \frac{\partial v_2^{(1)}}{\partial x^*} + u_2^{(1)}/2 = -\frac{\partial h_2^{(1)}}{\partial y^*} \quad (5.4b)$$

$$\frac{\partial}{\partial x^*} [(1 - (y^*)^2/8)u_2^{(1)} + h_2^{(1)}/2] = 0. \quad (5.4c)$$

The $O(\epsilon^2)$ balances are

$$\frac{\partial v_2^{(2)}}{\partial x^*} - \frac{\partial u_2^{(2)}}{\partial y^*} = 0 \quad (5.5a)$$

$$u_2^{(1)} \frac{\partial v_2^{(1)}}{\partial x^*} + \frac{\partial v_2^{(2)}}{\partial x^*} \left(\frac{y^*}{2}\right) - u_2^{(2)}/2 + u_2^{(2)} = -\frac{\partial h_2^{(2)}}{\partial y^*} \quad (5.5b)$$

$$\frac{\partial}{\partial x^*} \{[h_2^{(2)}y^*/2 + h_2^{(1)}/2]u_2^{(1)} + [1 - (y^*)^2/8]u_2^{(2)}\} = 0. \quad (5.5c)$$

The geometry of the section in the immediate vicinity of section 2 is shown in Fig. 8.

c. General solution for section 3

By substituting (4.15) into (4.6c) and eliminating the basic state, one obtains the equations,

$$\frac{\epsilon}{r^*} \frac{d}{dr^*} [r^* v_{\phi}^{(1)} + \epsilon r^* v_{\phi}^{(2)}] + O(\epsilon^3) = 0 \quad (5.7)$$

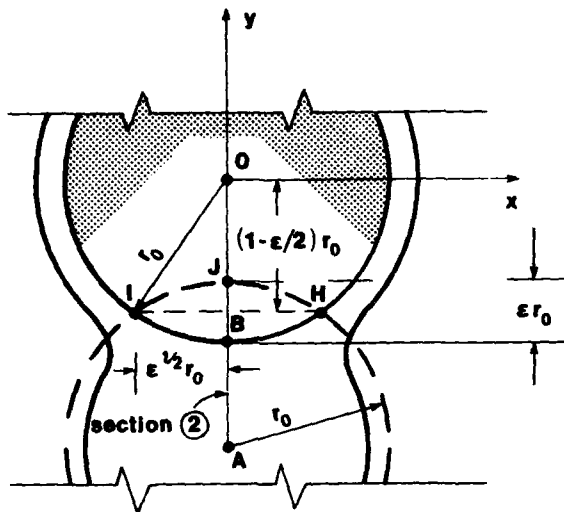


FIG. 8. The geometry in the vicinity of section 2.

$$0 = \epsilon \frac{dh_3^{(1)}}{dr^*} \tag{5.8}$$

It will become clear shortly that the term containing $v_{\phi 3}^{(2)}$ is actually $O(\epsilon)$ and not $O(\epsilon^2)$ so that it must be included in the $O(\epsilon)$ balance.

To simplify the structure of (5.7), it is recalled that the first-order flow (in section 3) takes place within a distance of $O(\epsilon)$ from the cylinder surface so that, as in Nof (1986a), one may introduce the transformation,

$$r^* = 2\sqrt{2}(1 + \epsilon\xi^*)$$

where $\xi^* \sim O(1)$. In terms of this new variable, (5.7) is,

$$\frac{1}{2\sqrt{2}} \frac{dv_{\phi 3}^{(1)}}{d\xi^*} + \epsilon \left[\frac{\xi^*}{2\sqrt{2}} \frac{dv_{\phi 3}^{(1)}}{d\xi^*} + v_{\phi 3}^{(2)} \right] + O(\epsilon^2) = 0$$

which shows that $dv_{\phi 3}^{(1)}/d\xi^* = 0$. This and (5.8) give,

$$v_{\phi 3}^{(1)} = B_3; \quad h_3^{(1)} = A_3 \tag{5.9}$$

where B_3 and A_3 are constants to be determined from the boundary conditions. Substitution of (5.9), (4.15), (5.2), (5.3) and (4.14) into the polar version of the boundary conditions (4.9) and (4.11) gives

$$\left[-\frac{\tilde{r}}{2} \right]_{\tilde{r}=2\sqrt{2}(1+\epsilon r_1^{(1)})} = \left[-r^*/2 + \epsilon B_3 \right]_{r^*=2\sqrt{2}(1+\epsilon r_3^{(1)})} \tag{5.10}$$

$$\left[1 - (r^*)^2/8 \right] + \epsilon A_3 = 0; \quad r^* = 2\sqrt{2}(1 + \epsilon r_3^{(1)}) \tag{5.11}$$

which, with the aid of (5.3b), yields,

$$B_3 = \sqrt{2}\gamma_3^{(1)}; \quad A_3 = 2\gamma_3^{(1)} \tag{5.12}$$

By now, most of the first-order solution for section 3 has been derived; the only part that is still missing is

$\gamma_3^{(1)}$. As we shall see, there are two equations and a boundary condition (4.10a) that we have not used yet. The latter immediately gives,

$$\sqrt{2}u_2^{(1)} = h_2^{(1)} \quad \text{at } y^* = -2\sqrt{2}. \tag{5.13}$$

d. The torque constraint

Since $(h_3^*) \sim O(\gamma_3) \sim O(\epsilon)$ it follows that the third integral in (4.13) is, at the most, $O(\epsilon^2)$. With the aid of the transformation $\tilde{y} = y^* + 2\sqrt{2}(2 - \epsilon)$ and (5.3b), the approximate form of (4.13) [up to $O(\epsilon^2)$] can be rewritten as

$$\int_{-2\sqrt{2}}^0 [\tilde{h}_1(\tilde{u}_1)^2 - \tilde{\psi}_1 + (\tilde{h}_1)^2/2][\tilde{y} - 2\sqrt{2}(2 - \epsilon)]d\tilde{y} + \int_0^{2\sqrt{2}-\epsilon} [\tilde{h}_2(\tilde{u}_2)^2 - \tilde{\psi}_2 + (\tilde{h}_2)^2/2] \times [\tilde{y} - 2\sqrt{2}(2 - \epsilon)]d\tilde{y} + O(\epsilon^2) = 0 \tag{5.14}$$

where, as before, the tilde ($\tilde{\quad}$) above the variables u , ψ and h indicates that they are expressed in terms of \tilde{x} , \tilde{y} . Substitution of (4.14), (4.17), (5.2) and (5.3) into (5.14) and elimination of the basic state gives,

$$\int_0^{2\sqrt{2}} [2\tilde{h}_2^{(0)}\tilde{u}_2^{(0)}\tilde{u}_2^{(1)} + (\tilde{u}_2^{(0)})^2\tilde{h}_2^{(1)} - \tilde{\psi}_2^{(1)} + \tilde{h}_2^{(0)}\tilde{h}_2^{(1)}](\tilde{y} - 4\sqrt{2})d\tilde{y} + \int_{2\sqrt{2}}^{2\sqrt{2}-\epsilon} [\tilde{h}_2^{(0)}(\tilde{u}_2^{(0)})^2 - \tilde{\psi}^{(0)} + (\tilde{h}_2^{(0)})^2/2](\tilde{y} - 4\sqrt{2})d\tilde{y} + O(\epsilon^2) = 0. \tag{5.15}$$

This equation can be further simplified by noting that the second integral is associated with the area where $\tilde{h}_2^{(0)} \sim O(\epsilon)$, and $\tilde{\psi}_2^{(0)} \sim O(\epsilon^2)$ so that it is, at the most, of $O(\epsilon^2)$. Hence, to $O(\epsilon)$, (5.15) reduces to

$$\int_0^{2\sqrt{2}} [2\tilde{h}_2^{(0)}\tilde{u}_2^{(0)}\tilde{u}_2^{(1)} + (\tilde{u}_2^{(0)})^2\tilde{h}_2^{(1)} - \tilde{\psi}_2^{(1)} + \tilde{h}_2^{(0)}\tilde{h}_2^{(1)}](\tilde{y} - 4\sqrt{2})d\tilde{y} + O(\epsilon^2) = 0$$

which, in terms of the x^* , y^* coordinates, is

$$\int_0^{-2\sqrt{2}} [2h_2^{(0)}u_2^{(0)}u_2^{(1)} + (u_2^{(0)})^2h_2^{(1)} - \psi_2^{(1)} + h_2^{(0)}h_2^{(1)}]y^* dy^* + O(\epsilon^2) = 0. \tag{5.16}$$

A solution satisfying (5.16), the boundary condition (5.13) and the governing equations (5.4a-c) is simply,

$$u_2^{(1)} = h_2^{(1)} = \psi_2^{(1)} = 0. \tag{5.17}$$

This leaves only one unknown, $\gamma_3^{(1)}$, which will be computed from the $O(\epsilon^2)$ balances.

e. The second-order balances

Two comments should be made before discussing the $O(\epsilon^2)$ equations. First, the $O(\epsilon)$ continuity equation

is automatically satisfied by the $O(\epsilon)$ solution that we have derived for section 2. Second, although the $O(\epsilon^2)$ continuity constraint involves the $O(\epsilon)$ variables in section 3, it also involves the $O(\epsilon^2)$ variables in section 2. In other words, as in Nof (1986a) it is necessary to find the $O(\epsilon^2)$ solution in sections 1 and 2 in order to obtain the $O(\epsilon)$ solution in section 3.

In view of this, we shall consider now the $O(\epsilon^2)$ potential vorticity equation, the momentum balance, and the local continuity balance for section 2 [Eqs. (5.5a-c)] which have the solution,

$$u_2^{(2)} = \delta \bar{y}; \quad \frac{\partial v_2^{(2)}}{\partial \bar{x}} = \delta; \quad h_2^{(2)} = -\delta y^2/2 \quad (5.18)$$

where δ is a constant to be determined.

This solution satisfies the boundary condition $u_2^{(2)} = v_2^{(2)} = h_2^{(2)} = 0$ at $x^* = y^* = 0$ as required. Together with the first- and second-order solutions for the various sections and the second-order solution for section 1 [relation (5.3c)], the second-order balance of the integrated continuity equation gives

$$1 + 2\delta = (\gamma_3^{(1)})^2. \quad (5.19a)$$

Similarly, the second-order balance of the integrated torque (4.13) yields

$$3.467\delta - 3 + (\gamma_3^{(1)})^2 = 0. \quad (5.19b)$$

Equations (5.19a) and (5.19b) have the solution,

$$\gamma_3^{(1)} = 1.316; \quad \delta = 0.366 \quad (5.19c)$$

This completes the derivation of the solution.

f. The complete solution

The total solution for section 1 is

$$\left. \begin{aligned} u_1^\dagger &= \bar{y}/2 + O(\epsilon^3) \\ h_1^\dagger &= [1 - (\bar{y})^2/8] + O(\epsilon^3) \\ v_1^\dagger &= 0 \\ \gamma_1 &= 0 + O(\epsilon^3) \end{aligned} \right\} \quad (5.20a)$$

In terms of the nontransformed coordinates [see (4.6b)], it takes the form,

$$\left. \begin{aligned} u_1^\dagger &= (y^* + 4\sqrt{2})/2 - \sqrt{2} \cdot \epsilon + O(\epsilon^3) \\ h_1^\dagger &= [1 - (y^* + 4\sqrt{2})^2/8] \\ &\quad + \epsilon(y^* + 4\sqrt{2})\sqrt{2}/2 - \epsilon^2 + O(\epsilon^3) \\ v_1^\dagger &= 0; \quad \gamma_1 = 0 + O(\epsilon^3) \end{aligned} \right\} \quad (5.20b)$$

where, as pointed out earlier, the terms of $O(\epsilon)$ in (5.20b) are not actual dynamical perturbations but rather a result of our choice for the origin of the coordinate system.

Similarly, the solution for section 2 is

$$\left. \begin{aligned} u_2^\dagger &= \bar{y}/2 + 0.366\bar{y}\epsilon^2 + O(\epsilon^3) \\ v_2^\dagger &= 0 \\ h_2^\dagger &= [1 - (\bar{y})^2/8] - 0.183(\bar{y})^2\epsilon^2 + O(\epsilon^3) \end{aligned} \right\} \quad (5.20c)$$

which in the (x^*, y^*) coordinates can be written as

$$\left. \begin{aligned} u_2^\dagger &= (y^* + 4\sqrt{2})/2 - \sqrt{2} \cdot \epsilon \\ &\quad + 0.366(y^* + 4\sqrt{2})\epsilon^2 + O(\epsilon^3) \\ h_2^\dagger &= [1 - (y^* + 4\sqrt{2})^2/8] \\ &\quad + \epsilon(y^* + 4\sqrt{2})\sqrt{2}/2 \\ &\quad - [0.183(y^* + 4\sqrt{2})^2 + 1]\epsilon^2 \\ &\quad + O(\epsilon^3) \\ v_2^\dagger &= 0 \end{aligned} \right\} \quad (5.20d)$$

For section 3, the solution is,

$$\left. \begin{aligned} u_3^\dagger &= -y^*/2 + 1.861\epsilon + O(\epsilon^2) \\ h_3^\dagger &= 1 - (y^*)^2/8 + 2.632\epsilon + O(\epsilon^2) \\ \gamma_3^\dagger &= 1.316\epsilon + O(\epsilon^2) \\ v_3^\dagger &= 0 \end{aligned} \right\} \quad (5.21)$$

Note that since γ_3^\dagger , the width of the intrusion around the cylinder, is not zero for $\epsilon \neq 0$ there *must* always be a flow around the cylinder as stated before. Due to the cylinder, part of the circulation in section 2 is blocked. Consequently, the flow intensifies near the cylinder surface and the portion of the eddy flux that is "blocked" (by the cylinder) is simply diverted from its original position to the perimeter of the solid cylinder. The solution demonstrates that, no matter how small the penetration of the cylinder into the vortex, a current engulfing the cylinder must always be present.

6. Laboratory experiments

To assess the weaknesses and limitations of the foregoing theory a set of simple laboratory experiments on a rotating table was performed. The lens-like eddy was formed on the bottom of a cylindrical tank by injecting dyed salty water through a tube (3 cm in diameter) containing a permeable foam. A cylinder (5 cm in diameter) was situated a distance of 5 cm away from the center of the tank where the injection tube was located.

First, the tank (45 cm in diameter) was filled to a height of 25 cm and rotated counterclockwise at a uniform rotation rate until the system reached a solid body rotation. The experiment began with the injection of the dyed salty water from the bottom. This formed a lens with a central height of a few centimeters. The lens slowly increased in size until it reached the edge of the cylinder when a cylinder-lens interaction took

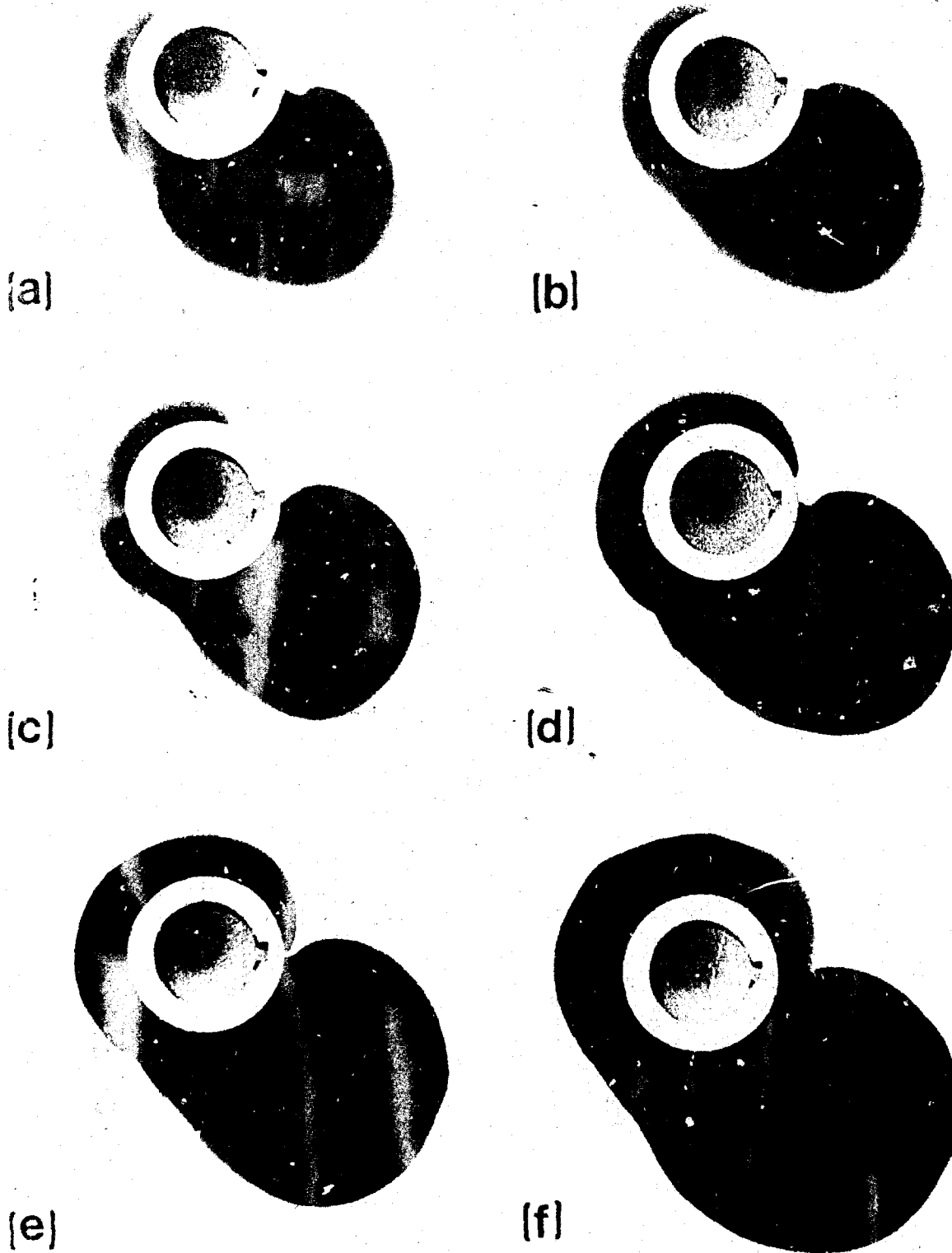


FIG. 9. Subsequent photographs of a (laboratory-generated) lens-like eddy responding to the presence of a solid cylinder. The sequence shows the structure of the eddy and the intrusion during the various stages of the interaction. Physical constants $f = 3.35 \text{ s}^{-1}$, $\Delta\rho/\rho = 1.0052$; $T = 21.5^\circ\text{C}$. The process shown in (a-f) lasted for about 20 seconds; the diameter of the cylinder is 5 cm. Note that, (i) a padlock flow is indeed established, as predicted by the theory, (ii) the eddy does not rotate around the cylinder, (iii) the lens remains roughly circular as assumed in the development of the theory, and (iv) during the interaction the eddy grows in time because of the continuous injection of dye/salty water through the bottom (see text).



FIG. 10. The coalescence of two quasi-geostrophic anticyclones in a two-layer basin (adapted from Griffiths and Hopfinger, 1987). Photographs were taken at the elapsed times shown on the counter (in background rotation periods). Coalescence begins at the first frame and ends in the second. The diameter of the eddies before the interaction was 18 cm; for other details see Griffiths and Hopfinger 1987. Note that, as the interaction begins, fluid from the blue vortex is engulfing the red vortex and that, ultimately, two adjacent spirals are formed as suggested by our model.

place. As can be seen in Fig. 9, the intrusion predicted by the theory (and shown in Fig. 6a) is clearly evident; also, the interaction clearly leads to a padlock flow as suggested by the theory (Fig. 6b).

It should be pointed out that, because of mechanical limitations, the injection could not be terminated during the actual execution of the experiment. Consequently, the lens continued to slowly grow in size during the interaction as is apparent in Fig. 9. This did not have a major effect on the results because the growth was small compared to a propagation speed of the intrusion. It should also be mentioned that, due to the fact that the upper layer was finite rather than infinite and due to the conservation of potential vorticity and angular momentum, a weak anticyclone was formed on top of the lens. Its influence on the interaction is probably minor because the ratio of the lens depth to the total depth was small (about 1/10) so that the speeds on top were also small.

7. General comments

Before discussing the application of our results to actual merging in the ocean, it is appropriate to comment on the "replacement" of one of the interacting eddies by a solid cylinder. An obvious similarity between a colliding eddy and a colliding cylinder is that both features are expected to exert a pressure on the eddy as they collide with it, and both features have similar geometry in the x - y plane. As we saw earlier, the exerted pressure is the key to the merging process and, therefore, it is believed that a solid cylinder provides an adequate "analog."

However, there are also some important differences between the solid cylinder and an actual eddy. For example, although both the actual eddy and the solid cylinder are subject to pressure forces, the former can adjust itself to the surrounding pressure, whereas the latter remains unaltered. In addition, as pointed out earlier, the actual eddy is drained via the intrusions so that a steady state is not reached before a complete merging is achieved.

While we should be on guard against oversimplified models (such as this one may seem, at first, to be), attacking the complete merging problem analytically appears to be hopeless. Even numerical integrations cannot provide the desired solution because of the difficulty in handling fronts ($\lambda = 0$). Some simplifications are, therefore, necessary and examination of the cylinder-eddy interaction is useful for understanding the basic processes in question. Namely, the results of our analytical study pinpoint the effects which one should look for in more complicated and more realistic models. It is worth pointing out that there is a similarity between our proposed merging mechanism (Figs. 3 and 4) and the laboratory observations of Griffiths and Hopfinger (1987) (see Fig. 10). Both include inter-

leaving spirals even though Griffiths and Hopfinger's (1987) experiments involved linear quasi-geostrophic eddies whereas our process addresses nonlinear lenses. As pointed out earlier, the main dynamical difference between these two kinds of eddies is that Griffiths and Hopfinger's eddies interacted *before* they touched each other whereas our vortices do not sense each other *unless a mutual boundary is established*. It should also be pointed out that the numerical experiments of McCreary and Kundu (1987) also suggest that merging takes place through the formation of intrusions and arms.

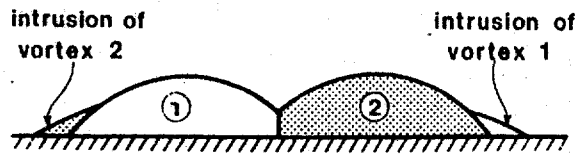
As far as the application of our general merging process to Cresswell's (1982) study is concerned, it appears that the essential dynamics may be similar. Because of the simplifications involved, a detailed quantitative comparison is, obviously, impossible. However, the fact that our model suggests a mechanism for eddy merging is, of course, in agreement with Cresswell's observations. The time scale for merging [relation (2.2) which gives ~ 30 days for $\epsilon = 0.1$ and $f \sim 10^{-4} \text{ s}^{-1}$] is also appropriate even though it is difficult to say what the actual value of ϵ should be.

A potentially serious difference between Cresswell's observations and the present study is the fact that Cresswell's eddies were with *unequal* densities whereas our model addresses eddies with identical densities. It is easy to see, however, that such a difference is not major because all that it implies is that the mean position of the intrusions along the rims will not be taking place on the same level. Instead, the mean position of the intrusions will take place on different levels as shown schematically in Fig. 11. The major cause of the merging—the establishment of a mutual boundary with a nonzero vanishing depth—is present in both the collision of eddies with equal densities and the collision of eddies with unequal densities. The laboratory experiments of Nof and Simon (1987) on eddies with unequal density support these considerations.

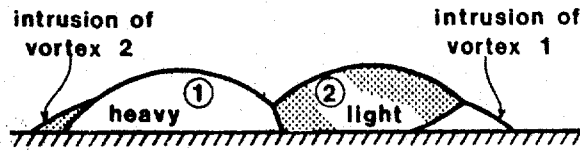
An additional aspect of Cresswell's study that is not present in our study is the observation of a clockwise migration of the entire eddies (Fig. 1). It is difficult to say what the causes of such an effect could be but it might be a result of the transient merging process which we have not studied in detail.

8. Summary

A conceptual qualitative model for the merging of two isolated lens-like eddies has been developed with the assumptions that: (i) the eddies are embedded in an infinitely barotropic fluid; (ii) with the exception of shock waves which are presumed to be present during the transient merging process, all motions are frictionless and hydrostatic; (iii) mass is conserved during the merging.



Eddies with equal densities



Eddies with unequal densities

FIG. 11. A cross section of pairing vortices. The upper panel shows eddies with identical densities; their merging is qualitatively displayed in Figs. 3 and 4. The lower panel displays eddies with unequal densities. While the merging is generated by the establishment of a mutual boundary with a nonvanishing depth as in the equal density case, the final situation is different from that displayed by Fig. 4a. Here, instead of forming two adjacent spirals, the lighter vortex is "climbing" on top of the heavier lens. This is supported by the laboratory experiments of Nof and Simon (1987).

Our attention has been focused on two lens-like eddies (with equal densities) which are pushed against each other by a mean flow that relaxes after the eddies are in contact. It is argued that the establishment of a "figure 8" structure (associated with a mutual boundary with a nonvanishing depth) forces the generation of "tentacles" and "arms." These features correspond to intrusions along the eddies' edges; they result from the fact that particles along the peripheries do not have sufficient energy to rise to the mutual nonzero depth (Fig. 2). The establishment of tentacles causes the eddies to wrap around each other (Fig. 3). As time goes on, the tentacles become longer and longer so that they effectively "drain" the vortices. Ultimately, a single vortex corresponding to two adjacent spirals is formed (Fig. 4).

While the details of the above process can be easily described in a qualitative manner, it is impossible to rigorously prove the complete process analytically because it is both nonlinear and three-dimensional (x, y, t). It is, however, possible to prove analytically that the establishment of tentacles is inevitable. To show this, we have conceptually replaced one of the interacting vortices by a solid cylinder (Figs. 5 and 6). This simplification removes the time dependency from the problem because there is now only one tentacle which, upon engulfing the cylinder, forms a steady "padlock"

flow. Using a constraint associated with the conservation of torque (i.e., moment of momentum) and a perturbation scheme, we have constructed the detailed solution even though the simplified problem is nonlinear. A set of laboratory experiments supports our analytical analysis of the padlock flow (Fig. 9).

With the aid of the above model, it has been shown that two lens-like eddies which are compressed against each other will merge within the period $\sim O(\epsilon^{5/2} f)^{-1}$ [where ϵ is the relative distance that each vortex is squeezed]. Following Nof and Simon (1987), it is speculated that during the merging the potential vorticity of penetrating oceanic vortices is altered via the action of shock waves near the nose of the tentacles. This is based on: 1) several studies (e.g., Griffiths 1986; Nof 1987) which have shown that transient intrusions contain breaking waves or shocks (bores) and 2) a recent study (Nof 1986b) which illustrated that shock waves cause major alterations in the potential vorticity. The details of the potential vorticity alteration by the action of shock waves in the intrusion is quite complicated and is beyond the scope of this study; it will be the focus of a future investigation. Finally, it should be pointed out that the observations of Griffiths and Hopfinger (1987) (Fig. 10) and the recent numerical experiments of McCreary and Kundu (1987) also illustrate that the merging of anticyclones takes place via the establishment of arms and tentacles.

Acknowledgments. This study was supported by the Office of Naval Research Contract N00014-C82-0404 and NSF Grant OCE871103. The laboratory experiments were supported by the Geophysical Fluid Dynamics Institute and the Department of Oceanography at Florida State University. Jim Winne assisted in the execution of the experiments. The comments of G. Cresswell on an earlier version of this paper are very much appreciated.

APPENDIX

List of Symbols

| | |
|------------|--|
| A_1, B_1 | Integration constants associated with (5.1) |
| A_3, B_3 | Integration constants associated with (5.7) and (5.8). Their relationship to $\gamma_3^{(1)}$ is given by (5.12). |
| b | Radius of eddy for energy calculations (section 1). |
| E | Total energy (kinetic plus potential). |
| f | The Coriolis parameter. |
| g' | "Reduced gravity" ($g\Delta\rho/\rho$ where g is the gravitational acceleration and $\Delta\rho$ is the density difference between the layers). |
| h | Maximum depth of vortex (i.e., depth at the point of no speed); it is also the maximum depth of the padlock flow at point A. |
| h_B | Depth at point B (Fig. 2). |

| | | | |
|--|---|------------|--|
| h^* | Nondimensional depth (h/\bar{h}). | | |
| i, f | Section 2—subscripts which denote the initial and final state (respectively). In section 3, "i" (1, 2, 3) denotes association with various sections (3.1). | α | a system whose origin is situated at the center of the solid cylinder. An integration constant associated with the solution of (4.1). |
| r | Radius in polar coordinates whose origin is located at the center of the solid cylinder. | γ_1 | Distance between the edge of the padlock flow (in section 1) and the edge of the undisturbed vortex (nondimensionalized by $2\sqrt{2}R_d$). |
| R_d | Deformation radius $(g'\bar{h})^{1/2}/f$. | γ_3 | Distance between the edge of the intrusion (in section 3) and the surface of the solid cylinder (nondimensionalized by $2\sqrt{2}R_d$). |
| r_0 | In section 3—radius of solid cylinder (Fig. 6b); in section 4 it is shown that, for our case, r_0 is also the radius of the undisturbed vortex, $2(2g'\bar{h})^{1/2}$. | δ | A nondimensional coefficient associated with the second-order flow in section 2. It is found to be equal to 0.366. |
| r^* | Nondimensional radius in a polar coordinates system with an origin at the center of the cylinder. | ϵ | In section 2—the distance that each vortex is "pushed" into the other (Fig. 2); in section 3—the distance between the edge of the undisturbed vortex and the edge of the cylinder (Fig. 6b). Note that the undisturbed vortex is defined as a zero potential vorticity lens which is aligned with the center and depth of the padlock flow (i.e., it has the same center and depth as the padlock flow). |
| $\tilde{r}, \tilde{\theta}$ | Nondimensional radius and angle in a polar coordinate system whose origin is located at the center of the undisturbed vortex (i.e., center of padlock flow). | ψ | Streamfunction. |
| t_m | Merging time. | ψ^* | Nondimensional streamfunction. |
| u_A, u_B | Speed along the x axis (i.e., in a Cartesian coordinates) for points A and B (Fig. 2). | \oint | Integration in a counterclockwise (clockwise) manner along a closed curve. |
| u, v | Speeds in Cartesian coordinates whose origin is located at the center of the solid cylinder (Fig. 6b). | | |
| u^*, v^* | Nondimensional speeds in Cartesian coordinates whose origin is located at the center of the solid cylinder (Fig. 6b). | | |
| $u^{(0)}, v^{(0)}, h^{(0)}$ | Velocity and depth (in Cartesian coordinates located at the center of the solid cylinder) of the undisturbed vortex. | | |
| $\tilde{u}^{(0)}, \tilde{v}^{(0)}, \tilde{h}^{(0)}$ | The undisturbed velocity and depth in a Cartesian coordinate system located at the center of the undisturbed vortex. | | |
| $u^{(1)}, v^{(1)}, h^{(1)}, u^{(2)}, v^{(2)}, h^{(2)}$ | First- and second-order perturbations to the basic flow (in Cartesian coordinates located at the center of the solid cylinder). | | |
| v_{oi} | Initial orbital speed in polar coordinates whose origin is situated at the center of the vortex. | | |
| \tilde{v}_o, \tilde{h} | Nondimensional orbital speed and depth in a polar coordinates whose origin is located at the center of the undisturbed vortex. The distance between the center of a point vortex and a wall (section 5). | | |
| x, y, t | Space and time coordinates in a Cartesian coordinates whose origin is situated at the center of the solid cylinder. | | |
| \tilde{x}, \tilde{y} | Space in a Cartesian coordinates located at the center of the undisturbed vortex (point A, Fig. 6b). It is related to x, y by, $y = \tilde{y}\sqrt{2}(2 - \epsilon)$; $x = \tilde{x}$. | | |
| x^*, y^* | Nondimensional Cartesian coordinates in | | |

REFERENCES

- Benjamin, T. B., 1968: Gravity currents and related phenomena. *J. Fluid Mech.*, **31**, 209-248.
- Cheney, R. E., 1977: Synoptic observations of the oceanic frontal system east of Japan. *J. Geophys. Res.*, **82**, 5459-5468.
- Christiansen, J. P., and N. J. Zabusky, 1973: Instability, coalescence, and fission of finite-area vortex structures. *J. Fluid Mech.*, **61**, 219-243.
- Cresswell, G. R., 1982: The coalescence of two East Australian Current warm-core eddies. *Science*, **215**, 161-164.
- , and R. Legeckis, 1987: Eddies off southeastern Australia, 1980/81. *Deep-Sea Res.*, **34**, 1527-1562.
- Gill, A. E., and R. W. Griffiths, 1981: Why should two anticyclonic eddies merge? *Ocean Modelling*, **41**, 10-16.
- Griffiths, R. W., 1986: Gravity currents in rotating systems. *Ann. Rev. Fluid Mech.*, **18**, 59-89.
- , and E. J. Hopfinger, 1983: Gravity currents moving along a lateral boundary in a rotating fluid. *J. Fluid Mech.*, **134**, 357-399.
- , and —, 1986: Experiments with baroclinic vortex pairs in a rotating fluid. *J. Fluid Mech.*, **173**, 501-518.
- , and —, 1987: Coalescing of geostrophic vortices. *J. Fluid Mech.*, **178**, 73-97.
- Kubokawa, A., and K. Hanawa, 1984: A theory of semigeostrophic gravity waves and its application to the intrusion of a density current along a coast. Parts I and II. *J. Oceanogr. Soc. Japan*, **40**, 247-270.
- Lai, D. Y., and P. L. Richardson, 1977: Distribution and movement of Gulf Stream rings. *J. Phys. Oceanogr.*, **7**, 670-683.
- McCreary, J., and P. Kundu, 1987: A numerical investigation of the

- Somali Current during the Southwest Monsoon. *J. Mar. Res.*, **46**, 25-58.
- McWilliams, J. C., 1983: Interactions of isolated vortices. II. Modon generation by monopole collision. *Geophys. Astrophys. Fluid Dyn.*, **24**, 1-22.
- , and N. J. Zabusky, 1982: Interactions of isolated vortices. I. Modons colliding with modons. *Geophys. Astrophys. Fluid Dyn.*, **19**, 207-227.
- Melander, M. V., N. J. Zabusky and J. C. McWilliams, 1986: A model for symmetric vortex-merger. Trans. Third Army Conf. on Appl. Mathematics and Computing. ARO Rep. 867.
- Mied, R. P., and G. J. Lindemann, 1984: Mass transfer between Gulf Stream Rings. *J. Geophys. Res.*, **89**, 6365-6372.
- Nof, D., 1986a: The collision between the Gulf Stream and warm-core rings. *Deep-Sea Res.*, **33**, 359-378.
- , 1986b: Geostrophic shock waves. *J. Phys. Oceanogr.*, **16**, 886-901.
- , 1987: Penetrating outflows and the dam-breaking problem. *J. Mar. Res.*, **45**, 557-577.
- , and L. Simon, 1987: Laboratory experiments on the merging of anticyclonic eddies. *J. Phys. Oceanogr.*, **17**, 343-357.
- Overman, E. A., and N. J. Zabusky, 1982: Evolution and merger of isolated vortex structures. *Phys. Fluids*, **23**, 2339-2342.
- Ring Group, 1981: Gulf Stream cold-core rings: Their physics, chemistry, and biology. *Science*, **212**, 1091-1100.
- Simpson, J. E., 1982: Gravity currents in the laboratory, atmosphere, and ocean. *Ann. Rev. Fluid Mech.*, **14**, 213-234.
- Stern, M. E., J. A. Whitehead and B. L. Hua, 1982: The intrusion of a density current along the coast of a rotating fluid. *J. Fluid Mech.*, **12**, 237-265.
- Young, W. R., 1985: Some interaction between small numbers of baroclinic geostrophic vortices. *Geophys. Astrophys. Fluid Dyn.*, **33**, 35-61.